

# Computational Laser Speckle Contrast Imaging in Endoscopic System

Guy Satat, Barmak Heshmat, Tristan Swedish, Ramesh Raskar

Media Lab, Massachusetts Institute of Technology, 77 Massachusetts Ave., 02139, Cambridge, MA, USA  
guysatat@mit.edu

**Abstract:** We demonstrate an endoscopic imaging system for microscopic flow measurement (for example blood flow in tissue) using laser speckle contrast imaging. Computational imaging is used to reject sub-surface scattering and eliminates erroneous flow speed estimation.

**OCIS codes:** (110.6150) Speckle imaging; (110.1758) Computational imaging; (170.2150) Endoscopic imaging

## 1. Introduction

When coherent light is scattered from a rough surface it interferes and results in a random high frequency pattern called speckle. The speckle encodes the random surface variations as small as the optical wavelength, regardless of the system magnification. One example that uses this encoding allows the measurement of flow or time dependent variations in the surface. This is known as laser speckle contrast imaging (LSCI) [1]. LSCI has found many applications in measuring tissue perfusion (blood flow into tissue), by measuring the average speed of red blood cells. LSCI benefits from simple hardware requirements (laser as a coherent source and a standard camera), and single shot acquisition which makes it appealing for challenging imaging environments such as endoscopic systems[2]. However, the technique provides only qualitative speed estimation.

Another main limitation of LSCI is model sensitivity that results in degradation of the recovered flow. We have previously demonstrated [3] a technique to mitigate some of these model-miss match by rejecting sub-surface scattering using computational technique. The proposed Computational LSCI allows qualitative improvement in skin perfusion measurements.

Here, we demonstrate that our computational scattering rejection framework for LSCI extends well into an endoscopic imaging system. We also present new results that clearly show how scattering rejection eliminates errors in flow speed reconstruction. This demonstration in an endoscopic system opens the door to challenging biomedical imaging applications and industrial inspection settings.

## 2. Methods

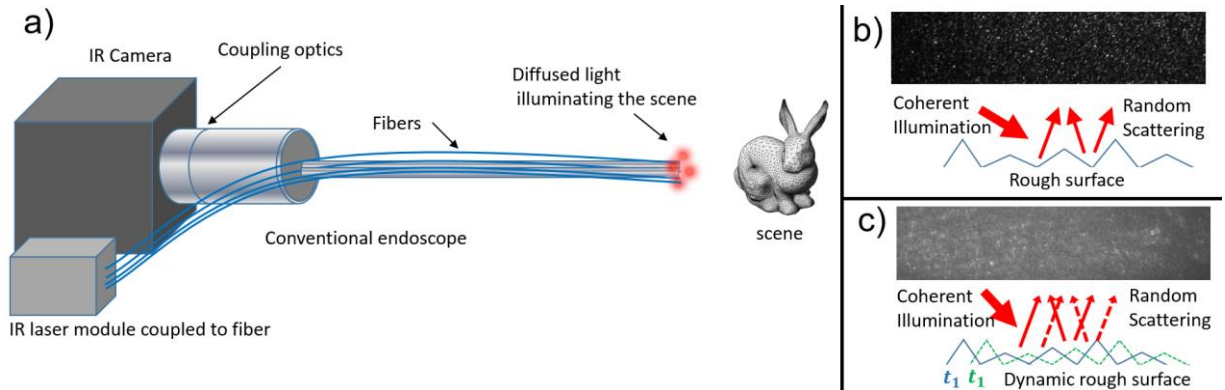


Figure 1. Computational endoscopic LSCI system. a) Schematic of our imaging system, the scene is sequentially illuminated by four lasers and imaged by a camera coupled to an endoscope. b) When the scene's surface is static the captured image contains high contrast speckle. c) When there is movement in the surface, the speckle's contrast reduces.

Our optical setup is presented in Fig. 1a. Similar to traditional LSCI systems we use a standard camera (Pointgrey Chameleon monochrome) and a diffused laser source (Thorlabs 5mW 780nm laser pointer). Two key aspects differentiate our setup from traditional systems: first, the camera observes the target through an endoscope (Olympus 5 Series Rigid Borescope). Second, we sequentially illuminate the scene with four sources, and capture the corresponding four images. Thus, unlike standard LSCI systems that require a single image, we capture four images to calculate the flow, this helps in rejecting flow reconstruction errors.

LSCI is based on the high contrast speckle pattern that is formed when light is scattered from a rough surface (Fig. 1b). When there is movement in the surface during the exposure time, the camera integrates over multiple speckle patterns, and the pattern's contrast is reduced (Fig. 1c). Analysis of speckle is usually done from a statistical perspective. The goal is to measure the movement's characteristic timescale (denoted by  $\tau_c$ ) from the contrast [4]:

$$K = \sqrt{\frac{\tau_c}{2T} \left( 2 - \frac{\tau_c}{T} \left( 1 - \exp\left(-\frac{2T}{\tau_c}\right) \right) \right)} \quad (1)$$

here  $K$  is the contrast, and  $T$  is the camera exposure time. It is common [4] to approximate Eq. 1 and correlate  $\tau_c$  to the speed  $V$  such that:

$$V(r) \sim \frac{1}{TK(r)^2} \quad (2)$$

where we also added spatially varying speed and contrast (spatial coordinate  $r$ ). In order to calculate the local contrast we can take a high resolution image and calculate per pixel  $[i, j]$  the local mean  $\mu$  and local standard deviation  $\sigma$ :

$$K_{i,j} = \frac{\sigma_{i,j}}{\mu_{i,j}} \quad (3)$$

Calculation of the mean and standard deviation is accomplished by assuming the target is ergodic in spatial coordinates and using empirical estimation with neighboring pixels (we use a neighborhood of  $N = 9 \times 9$  pixels).

One way to improve speed reconstruction is to reject unwanted scattering (i.e. input the LSCI algorithm with an image that better meets the algorithm assumptions); for this purpose we utilize computational imaging to reject scattering. Fig. 2a shows various light paths that contribute to unwanted scattering. The scene radiance can be expressed by direct and global components. The direct component corresponds to single scattering (direct reflection that follow the path: source – scene – sensor). The global component is all other light paths that include more than one scatter events within the scene, for example inter reflections and sub-surface scattering.

Traditional global-direct separation [5] is accomplished by projecting multiple high frequency patterns, and capturing the corresponding images. These multiple images are used to computationally construct two images for the direct and global components whose weighted sum is equal to a standard image of the scene. For our purpose we only require the direct component which is given by:

$$D_{i,j} = \frac{L^+_{i,j} - L^-_{i,j}}{1 - b} \quad (4)$$

Where  $L^+_{i,j}$  and  $L^-_{i,j}$  are pixel wise maximum and minimum across the captured images. And,  $b$  is a constant that accounts for background illumination. We note that speckle is a natural high frequency pattern, so it acts as the high frequency illumination pattern in our case.

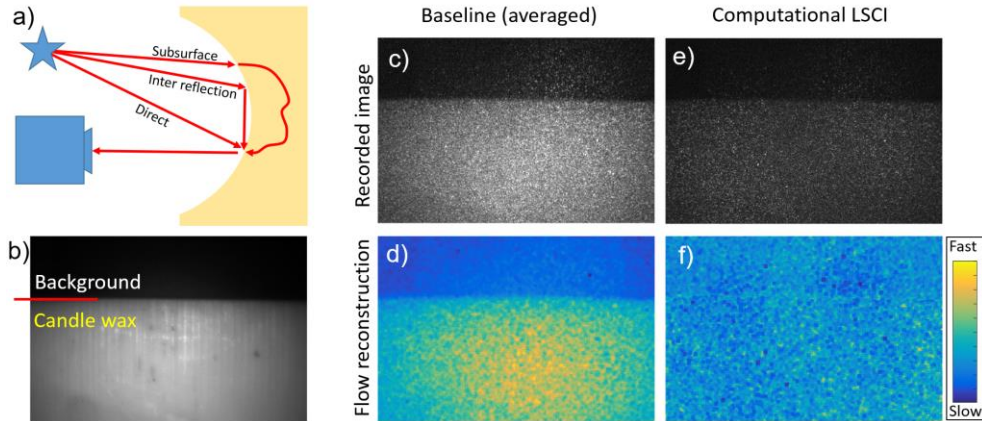


Figure 2. Effects of scattering on LSCI. a) Schematic of various light paths in a scene. The direct component is a single reflection, the global component includes indirect light paths. b) Photograph of candle wax target. c) Average of input speckled images used for LSCI flow estimation, serving as a baseline. d) Flow reconstruction for baseline shows significant speed on the static candle. e) Result of direct component extraction. f) LSCI output for the direct component correctly shows zero flow.

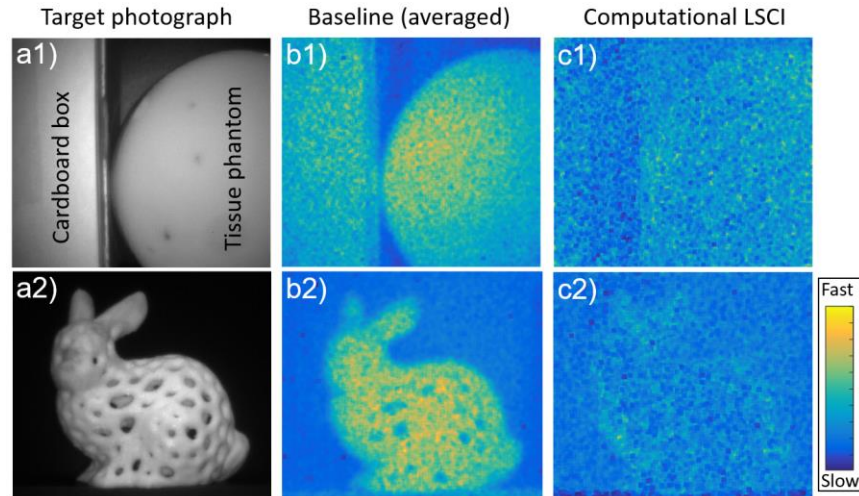


Figure 3. Computational LSCI removes flow reconstruction errors. Two targets are demonstrated, top: a tissue phantom next to a cardboard box, bottom: a 3D printed model of a rabbit. a) Photograph of target. b) Baseline flow reconstruction shows corrupted speed distribution on a static target. c) Flow reconstruction using the direct component correctly produces zero speed distribution.

To summarize, Computational LSCI follows these steps: (1) capture four images, each taken with a different laser source illuminating the scene. (2) Calculate the direct component image (Eq. 4). (3) Calculate the speed map using the LSCI algorithm (Eq. 2,3) on the direct component image.

### 3. Results

Fig. 2b shows a target scene of a static candle (the candle wax causes significant subsurface scattering). In order to evaluate our method we use a baseline in which we perform the LSCI algorithm on the individual four images and take the mean of the results. The scene is completely static and we expect to measure zero speed. However, when using the traditional LSCI approach (baseline) the border of the candle is very obvious and we get significant speed distribution on the static candle. On the contrary, when using just the direct component, the candle border is undistinguishable (i.e. the background and candle show the same zero speed distribution as required). Notice that the baseline input image shows significant glow as a result of the subsurface scattering.

In Fig. 3 we perform similar analysis on a tissue phantom target and a cardboard box (top row), both are static without any flow. We expect both objects to show zero speed distribution. However, the expected result is observed only when using just the direct component. In the baseline result, the cardboard box that causes little subsurface scattering shows near zero speed. In contrast, the tissue phantom which contributes to significant subsurface scattering shows erroneous high speed distributions. Computational LSCI correctly produces a zero speed map.

Corruption of the speed map can also be caused by inter reflections. Fig. 3 bottom shows an example of such a case, demonstrated with a 3D printed shape of a rabbit. The complicated surface causes many inter reflections in the scene. Similarly to previous examples, the standard LSCI approach reconstructs an erroneous non-zero speed map of the static scene, while using the direct component leads to a correct result.

### 4. Conclusions

We demonstrate computational LSCI, a novel method for flow measurement, in an endoscopic system. Our system is based on speckle contrast imaging for speed analysis, which is improved by a computational framework for unwanted scattering rejection. Several scenes with different types of scattering demonstrate that the use of standard LSCI results in erroneous non-zero speed map of a static scene, while our computational approach produces the correct zero-speed distribution. Our results also show that imaging with an endoscope is a viable option for flow imaging with various biomedical and industrial inspection applications.

### References

- [1] F. A. Fercher and J. D. Briers, "Flow visualization by means of single-exposure speckle photography," *Optics Communications*, 1981.
- [2] L. Song and D. Elson, "Endoscopic laser speckle contrast imaging system using a fibre image guide," in *Proc. of SPIE*, 2011.
- [3] G. Satat, C. Barsi, and R. Raskar, "Skin perfusion photography," in *IEEE International Conference on Computational Photography*, 2014.
- [4] J. Senarathna, A. Rege, N. Li, and N. V Thakor, "Laser Speckle Contrast Imaging: theory, instrumentation and applications.," *IEEE reviews in biomedical engineering*, 2013.
- [5] S. K. Nayar, G. Krishnan, M. D. Grossberg, and R. Raskar, "Fast separation of direct and global components of a scene using high frequency illumination," *ACM Transactions on Graphics*, 2006.